

A THERMO-ECONOMIC COMPARISON OF THE UP-THERM HEAT CONVERTER AND AN ORGANIC RANKINE CYCLE HEAT ENGINE

Kirmse C.J.W., Oyewunmi O.A., Haslam A.J. and Markides C.N.*

*Author for correspondence

Clean Energy Processes (CEP) Laboratory,
Department of Chemical Engineering,
Imperial College London,
London SW7 2AZ,
United Kingdom,
E-mail: c.markides@imperial.ac.uk

ABSTRACT

In this paper we compare a recently proposed two-phase thermofluidic oscillator device termed 'Up-THERM' to a basic (sub-critical, non-regenerative) equivalent organic Rankine cycle (ORC) engine. In the Up-THERM heat converter, a constant temperature difference imposed by an external heat source and sink leads to periodic evaporation and condensation of the working fluid, which gives rise to sustained oscillations of pressure and volumetric displacement. These oscillations are converted in a load arrangement into a unidirectional flow, which passes through a hydraulic motor that extracts useful work from the device. A pre-specified Up-THERM design is being considered in a selected application with two *n*-alkanes, *n*-hexane and *n*-heptane, as potential working fluids. One aim of this work is to evaluate the potential of this proposed design. The thermodynamic comparison shows that the ORC engine outperforms the Up-THERM heat converter in terms of power output and thermal efficiency, as expected. An economic comparison, however, reveals that the capital costs of the Up-THERM are lower than those of the ORC engine. Nevertheless, the specific costs (per unit power) favour the ORC engine due to its higher power output. Some aspects of the proposed Up-THERM design are identified for improvement.

INTRODUCTION

Finite fossil-fuel reserves and the increased release of combustion emissions into the atmosphere over the last century have favoured the development of alternative energy conversion technologies, which can utilize low- and medium-grade heat, therefore increasing primary energy efficiency. 'Thermofluidic oscillators' are one particular class of promising heat conversion technologies that can contribute to this aim. This includes single-phase thermofluidic oscillators, such as Sondhauss tubes [1], thermoacoustic engines [2], Fluidyne engines [3], and also the two-phase 'Non-Inertive-Feedback Thermofluidic Engine' (NIFTE) [4–7]. In this paper we present the 'Up-THERM' heat converter. The Up-THERM is an alternative two-phase thermofluidic oscillator, which is similar in operation to the NIFTE engine and additionally contains a single solid piston [8].

By applying and maintaining, with an external heat source and

sink, a constant temperature difference between hot and cold heat exchangers, the working fluid inside the Up-THERM converter evaporates and condenses periodically as the working fluid oscillates within the device. This gives rise to sustained reciprocating vertical motions of the solid piston and sustained oscillations of pressure, temperature and liquid volume. The oscillating volumetric displacement is turned into a uni-directional flow of a liquid in a hydraulic load arrangement. Power can then be extracted from the cycle by this liquid flow through a hydraulic motor.

In this paper we compare a pre-specified Up-THERM design with two *n*-alkanes, *n*-hexane and *n*-heptane, as potential working fluids in a selected application, to a more mature heat-conversion technology namely an equivalent basic (sub-critical, non-regenerative) organic Rankine cycle (ORC) engine. Although it is expected that the Up-THERM will, generally, have inferior performance to the ORC engine, its costs will also be considerably lower since the Up-THERM has few moving parts and dynamic seals, and can be constructed with low-cost manufacturing techniques and materials. Therefore, beyond the comparison of key thermodynamic indicators, such as power output, exergy efficiency and thermal efficiency, we perform a simple economic analysis of both engines by evaluating the bare module costs and the specific costs (per unit power) to give an indication of the cost effectiveness of the novel Up-THERM heat converter.

METHODOLOGY

Up-THERM Engine Operation

A schematic of the Up-THERM heat converter is shown in Fig. 1. The heat converter comprises a vertical displacer cylinder (left hand side of Fig. 1 and inset), a connection tube, and a load ensemble including a hydraulic motor, two hydraulic accumulators and two check valves. The operation of the Up-THERM heat converter is described briefly below; a more extensive description is available in Kirmse et al. [9] and Oyewunmi et al. [10].

Considering a cycle starting with the piston at top dead centre (TDC) as depicted in Fig. 1, the piston valve is open, the mechanical spring is fully extended, and the vapour-liquid interface is in contact with the hot heat exchanger. Evaporation of the liquid working fluid causes the pressure in the vapour-space gas spring

NOMENCLATURE

A	[m ²]	Area
B	[-]	Constant
C	[m ⁴ s ² /kg, £]	Capacitance, Cost
c_i	[-]	Geometric constants ($i = 1, 2, 3$)
d	[m]	Diameter
F	[-]	Factor
g	[m/s ²]	Gravitational acceleration
H	[m]	Head
h	[W/(m ² K), kJ/kg]	Heat transfer coefficient, Specific enthalpy
K	[-]	Constant
k	[N/m]	Spring constant
L	[kg/m ⁴]	Inductance
l	[m]	Length
m	[kg]	Mass
P	[Pa]	Pressure
\dot{Q}	[W]	Heat flow rate, thermal power
R	[kg/(m ⁴ s)]	Resistance
T	[°C, K]	Temperature
t	[s]	Time
U	[m ³ /s]	Volumetric flow rate
V	[m ³]	Volume
\dot{W}	[W]	Power
\dot{X}	[W]	Exergy flow rate
Greek		
α	[°C, K]	Temperature amplitude
β	[1/m]	Temperature profile parameter
γ	[-]	Heat capacity ratio
δ	[m]	Gap between piston and slide bearing
η	[%]	Efficiency
μ	[kg/(ms)]	Dynamic (absolute) viscosity
ρ	[kg/m ³]	Density
Subscripts and Superscripts		
0		Equilibrium/base/time-average state conditions
1		ORC condenser outlet/pump inlet state conditions
2		ORC pump outlet/evaporator inlet state conditions
3		ORC evaporator outlet/expander inlet state conditions
4		ORC expander outlet/condenser inlet state conditions
BM		Bare module
b		Slide bearing
C		Carnot
c		Connection tube
cv		Check (non-return) valve
el		Electrical
ex		Exergy
exp		Expander
gen		Power generating
hm		Hydraulic motor
hx		Heat exchanger
in, out		Into the cycle, Out of the cycle
LM		Log mean
l		Liquid, liquid-phase
lub		Lubricant
min, max		Minimum, Maximum
ms		Mechanical spring
p		Piston (solid)
pr		Pressure
pump		Pump
pv		Piston valve
s		Isentropic
sh		Shaft
ss		Stainless steel
t		Overall/total
th		Thermal
v		Displacer cylinder gas spring
wfl		Working fluid

to increase, which together with the mechanical spring (and less so, gravity), act to force the vapour-liquid interface downwards. With the piston valve closed, liquid is prevented from leaving the chamber above it while the piston continues its downward movement and the pressure above the piston valve increases further (the pressure below stays almost constant). After a certain downward displacement of the piston, the piston valve opens, liquid rushes from the upper to the lower chamber, and the pres-

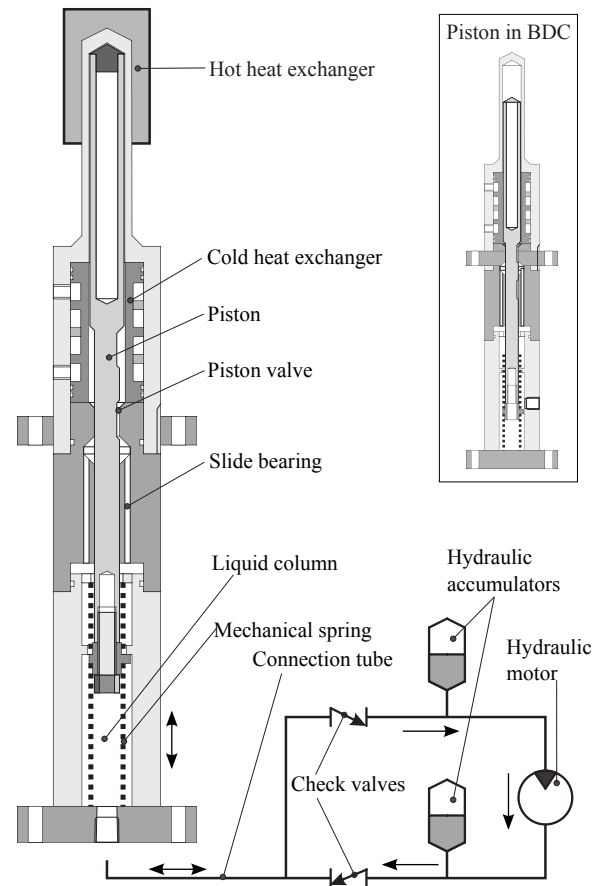


Figure 1. Schematic of the Up-THERM heat converter.

ures above and below the piston valve are suddenly equalized.

At this point the vapour-liquid interface comes into contact with the cold heat exchanger and working fluid in the vapour phase begins to condense. The piston valve closes, which creates a reduced pressure in upper chamber. This pressure difference together with the mechanical spring force the piston upwards. The valve opens again, liquid working fluid flows from the lower to the upper chamber, and the vapour-liquid interface comes into contact with the hot heat exchanger completing one cycle.

The aforementioned oscillating fluid movement in the displacer cylinder, and connection tube, is converted through the two check valves into a unidirectional flow through the hydraulic motor. The two hydraulic accumulators dampen the oscillating amplitudes of pressure and volumetric displacement. Power can be extracted from the cycle at the hydraulic motor.

Up-THERM Engine Model

The methodology used for the modelling of the Up-THERM heat converter follows earlier approaches by Huang and Chuang [11], Backhaus and Swift [12, 13], and, in particular, the framework used in modelling the NIFTE [5–7, 14] that showed good agreement with experimental data. The latter is considered a suitable starting point, also because the Up-THERM and NIFTE are both thermofluidic devices that feature phase-change heat exchange between the hot/cold heat exchangers and the working fluid.

The dominant fluid or thermal process in each component of

the Up-THERM is described by a spatially lumped ordinary differential equation (ODE). Assuming small variations around an operational equilibrium point, enables us to linearize the ODEs in the following components: liquid column; connection tube; piston; slide bearing; hydraulic accumulators; and, hydraulic motor. Electrical analogies are made such that thermal resistance or fluid drag are represented by resistors (R), liquid inertia by inductors (L), and vapour compressibility or hydrostatic pressure by capacitors (C). The pressure difference ΔP across a component and the volume flow rate U through it can be related via Ohm's, Faraday's and Gauss's laws by the first-order ODEs:

$$\Delta P = RU; \quad \Delta P = L \frac{dU}{dt}; \quad \frac{d(\Delta P)}{dt} = \frac{1}{C} U. \quad (1)$$

In particular, quasi-steady, fully developed laminar flow is assumed in the liquid columns, as the Reynolds and Womersley numbers are sufficiently low. Thus, by simplifying the governing (Navier-Stokes) equation of this flow, the following R , L and C descriptions are derived, corresponding to Eq. (1):

$$R = \frac{128\mu l_0}{\pi d^4}; \quad L = \frac{4\rho l_0}{\pi d^2}; \quad C = \frac{\pi d^2}{4\rho g}. \quad (2)$$

Hydrostatic pressure is negligible in the connection tube, and only the flow drag and liquid inertia are needed in the description of this flow. The piston and surrounding working fluid, including the slide bearing where the piston and flow are separated, are modelled by merging similar simplified equations as in Eqs. (1&2) for the annular liquid flow around the piston with a force balance on the piston. The following components emerge:

$$R_{l,I} = \frac{128c_2 l_p \mu}{\pi c_1 c_3}; \quad R_{l,II} = \frac{128c_2 l_p \mu}{\pi c_1 (c_1 - 2c_2 d_p^2)}; \quad R_p = \frac{64 l_p \mu}{\pi d_p^2 c_1};$$

$$R_{b,p} = \frac{16\mu l_b}{\pi^2 d_p^3 \delta}; \quad R_{b,l} = \frac{128\mu l_b}{\pi d_{b,l}^4}; \quad L_p = \frac{32m_p c_2}{\pi^2 d_p^2 c_1}; \quad (3)$$

$$L_{b,l} = \frac{4\rho l_b}{\pi d_b^2}; \quad L_1 = \frac{64c_2^2 m_p}{\pi^2 c_1 (c_1 - 2c_2 d_p^2)}; \quad L_{b,p} = \frac{4\rho_{ss} l_b}{\pi d_p^2};$$

$$C_p = \frac{\pi^2 d_p^2 c_1}{32k_{ms} c_2}; \quad C_1 = \frac{\pi^2 c_1 (c_1 - c_2 d_p^2)}{64c_2^2 k_{ms}},$$

with $c_1 = d_c^2 - d_p^2$, $c_2 = \ln(d_c/d_p)$, and $c_3 = c_2(d_c^2 + d_p^2) - c_1$.

The hydraulic accumulators are modelled as adiabatic (and reversible) gas springs filled with an ideal gas, with:

$$C = \frac{V_0}{\gamma P_0}. \quad (4)$$

Losses and inertia in the hydraulic motor are modelled by applying a torque balance to this component. The power that can be extracted from the cycle is dissipated in the load resistance R_{gen} , which is determined empirically in order to maximize power:

$$R_{hm} = \frac{16\mu_{lub} d_{sh}^3 l_{sh}}{\pi \epsilon d^4 d_{hm}^2}; \quad L_{hm} = \frac{8m_{hm}}{\pi^2 d^4}; \quad \dot{W}_{hm} = R_{gen} U_{hm}^2. \quad (5)$$

In addition to the (linear) description of the above mentioned components, the processes in some components are described non-linearly. The temperature profile along the heat exchanger wall is assumed to follow a hyperbolic tangent function [9]:

$$T_{hx}(y) = \alpha \tanh(\beta y), \quad (6)$$

where y is the vertical displacement of the vapour-liquid interface

from the equilibrium (time-mean) position.

Flow through the piston valve also exhibits an inherently non-linear behaviour, as the valve can only be either open (TDC and BDC) or closed (otherwise). This behaviour is described by the combination of two Heaviside step functions:

$$R_{pv} = R_{min} + \frac{1}{2} R_{max} (-H\{P_{l,d} - P_{pv}\} + H\{P_{l,d} + P_{pv}\}), \quad (7)$$

where $P_{pv} = \rho_{wfl} g l_{pv}$ is the position, described as a hydrostatic pressure, where the valve opens or closes.

The check (non-return) valves in the load arrangement open and close depending on the flow rate U_{cv} through them:

$$R_{cv} = R_{max,cv} H\{U_{cv}\}. \quad (8)$$

Finally, the working-fluid vapour-phase gas spring at the top of the displacer cylinder is assumed to be isentropic as with the accumulator gas springs, so that $PV^\gamma = \text{const.}$, but this is not linearized as is done in Eq. (3) for the latter. Hence, the pressure variations in the gas spring are described by:

$$\frac{dP_v}{dt} = \frac{\gamma P_v}{V_v} U_v. \quad (9)$$

Solving the (dynamic) Up-THERM engine model requires the specification of all RLC values in Eqs. (2-9), and of the parameters α , β that define the heat exchanger wall temperature profile in Eq. (6); see Section "Application Specification and Solution".

ORC Model

A schematic of the ORC engine that is used in this work is shown in Fig. 2. As is the case with the Up-THERM heat converter, the working fluid of the ORC remains in the sub-critical region. A simple layout without regeneration is selected for this comparison [15]. The liquid working fluid is pumped from State 1 to State 2 by the pump, which requires power \dot{W}_{pump} :

$$\dot{W}_{pump} = \dot{m}_{wfl} (h_{2s} - h_1) / \eta_{s,pump}, \quad (10)$$

with an isentropic efficiency $\eta_{s,pump}$ of 75%.

In the evaporator heat \dot{Q}_{in} from the heat source is transferred to the working fluid. The evaporator is assumed isobaric, without heat losses and with a minimum pinch ΔT of 10 °C:

$$\dot{Q}_{in} = \dot{m}_{wfl} (h_3 - h_2). \quad (11)$$

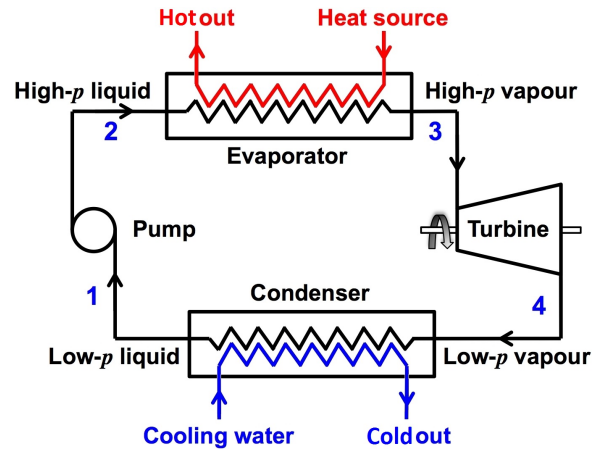


Figure 2. Simple schematic of the main components of the subcritical, non-regenerative ORC engine.

Finally, mechanical power is generated in the expander:

$$\dot{W}_{\text{exp}} = \eta_{\text{s,exp}} \dot{m}_{\text{wfl}} (h_{4\text{s}} - h_3). \quad (12)$$

with an isentropic efficiency $\eta_{\text{s,exp}}$ of 75%. The ORC engine is optimised for maximum net power output subject to the pinch conditions in the heat exchangers, the maximum pressure, which should be lower than 90% of the critical pressure, and the minimum pressure, which should not be below 1 bar.

Application Specification and Solution

Based on a given specification for the employment of an Up-THERM heat converter as a CHP prime-mover (suggested in the testing procedure of a prototype Up-THERM engine), the heat source temperature is set to 360 °C and the mass flow rate of the heat transfer fluid (thermal oil) that acts as the external heat source to the device is set to 1 kg/s. To enable a fair thermodynamic comparison between the two systems, the same heat source temperature and input thermal power into the two engines is used, although the heat input is allowed to vary when using different working fluids by adjusting a limited number of parameters that define the hot heat exchanger (specifically, the number, length and thickness of external fins in contact with a heat transfer fluid). The heat sink temperatures are also matched by specifying a cooling water flow rate at 10 °C. Similarly, the physical dimensions of the Up-THERM engine are taken from the same prototype design, and are fully specified in Kirmse et al. [9].

The physical dimensions of the Up-THERM heat converter along with the working fluid properties define all *RLC* model parameters, which can be calculated from Eqs. (2-9), as well as parameter β in Eq. (6) [9]. Finally, the heat source and heat sink conditions define parameter α , which is simply half of the difference between the heat source and sink temperatures, and therefore the heat exchanger wall temperature profile in Eq. (6).

Thermodynamic Performance Indicators

The thermodynamic performance indicators for the Up-THERM that are used in the current comparison are, beyond the power output as defined in Eq. (5), the device exergy efficiency and the thermal efficiency:

$$\eta_{\text{ex}} = \frac{\int R_{\text{gen}} U_{\text{hm}} dV_{\text{hm}}}{\int P_{\text{th}} dV_{\text{th}}}; \quad \eta_{\text{th}} = \frac{\dot{W}_{\text{hm}}}{\dot{Q}_{\text{in}}}, \quad (13)$$

where $V_{\text{hm}} = \int U_{\text{hm}} dt$ is the volume displacement over one cycle in the hydraulic motor, $V_{\text{th}} = \int U_{\text{th}} dt$ is the referred entropy flow to the working fluid due to heat transfer during one cycle, and $\dot{Q}_{\text{in}} = h A_{\text{hx,wfl}} (T_{\text{hx}} - T_{\text{wfl}})$ is the heat input into the cycle over half a cycle, with $A_{\text{hx,wfl}}$ the area of the heat exchanger that is in contact with the working fluid during the heat addition stage.

Similarly, the ORC engine thermal and exergy efficiencies are:

$$\eta_{\text{th}} = \frac{\dot{W}_{\text{exp}} - \dot{W}_{\text{pump}}}{\dot{Q}_{\text{in}}}; \quad \eta_{\text{ex}} = \frac{\dot{W}_{\text{exp}} - \dot{W}_{\text{pump}}}{\dot{X}_{\text{in}}}, \quad (14)$$

where \dot{Q}_{in} and \dot{X}_{in} are the heat and exergy input to the cycle.

Economic Performance Indicators

In order to estimate the capital costs of the two systems, the size of the heat exchangers of the Up-THERM and the ORC engines must be determined. A double-pipe heat exchanger is chosen for both engines. The area of the heat exchangers are calculated

according to Hewitt et al. [16] from:

$$A_t = \frac{\dot{Q}_{\text{in}}}{h_t \Delta T_{\text{LM}}}, \quad (15)$$

with an overall heat transfer coefficient h_t , a shell-side heat exchanger area A_t , which can include fins, and a logarithmic mean temperature difference T_{LM} . In the calculation of the area the hydraulic pump work required to pump the heat transfer fluid should not exceed 100 W, which corresponds to a pressure drop smaller than 1 bar in the heat exchanger.

For the Up-THERM, the area of the cold heat exchanger is assumed to have the same size as the hot heat exchanger. In order to calculate the major equipment costs a concept study according to Ref. [17] is performed. Based on this method, the bare module costs C_{BM} are calculated, which include the direct and indirect costs for a specific piece of equipment [17]:

$$C_{\text{BM}} = C_p^0 F_{\text{BM}}, \quad (16)$$

with C_p^0 the purchased cost for base conditions and F_{BM} the bare module factor that takes the material and operating pressure into account. For carbon steel at atmospheric pressure the purchased cost of equipment for base conditions is [17]:

$$\log(C_p^0) = K_1 + K_2 \log(A) + K_3 [\log(A)]^2, \quad (17)$$

where $K_1 = 3.3444$, $K_2 = 0.2745$ and $K_3 = 0.0472$ are constants that depend on the equipment and A is the heat exchanger area. The bare module factor can be calculated from [17]:

$$F_{\text{BM}} = B_1 + B_2 F_M F_{\text{pr}}, \quad (18)$$

where F_M is the material factor and F_{pr} the pressure factor. For double-pipe heat exchangers $B_1 = 1.74$ and $B_2 = 1.55$. The material of the heat exchangers is stainless steel, so that $F_M = 2.75$. For pressures under 40 bar, which is not exceeded in either engine and for any working fluid, F_{pr} is set to unity.

Finally, as the reference year for the calculations is 2001, the effect of inflation has to be taken into account. This is done by using the Chemical Engineering Plant Cost Index (CEPCI) [19]:

$$C_{\text{BM},2014} = C_{\text{BM},2001} \frac{\text{CEPCI}_{2014}}{\text{CEPCI}_{2001}}, \quad (19)$$

where $C_{\text{BM},2001} = 363.9$ and $C_{\text{BM},2014} = 640.7$.

For the hydraulic accumulators, the hydraulic motor and the displacer cylinder no cost correlations are available. For those pieces of equipment commercially available products, along with their market prices, are selected.

A positive displacement pump is chosen for the ORC engine due to the low pumping power required. A relation similar to Eq. (17) is used to calculate the pump cost, with the constants replaced by $K_1 = 3.48$, $K_2 = -0.135$ and $K_3 = 0.144$, and A being the pump power. The pump also requires an electric motor, whose cost is calculated according to [18]:

$$C_{\text{BM},2006} = \exp\{5.8259 + 0.13141 [\ln(\dot{W}_{\text{pump}})] + 0.053255 [\ln(\dot{W}_{\text{pump}})]^2 + 0.028628 [\ln(\dot{W}_{\text{pump}})]^3 - 0.0035549 [\ln(\dot{W}_{\text{pump}})]^4\}. \quad (20)$$

For the calculation of the expander cost the following expression is used, which has been derived from a survey of scroll expander manufacturers' data sheets and price lists:

$$\log(C_{\text{BM},2014}) = 3.819 + 0.5422 \log(\dot{W}_{\text{exp}}). \quad (21)$$

The currency Pound Sterling (£) is chosen for the economic evaluations in the present study. For equipment whose costs are only available in US Dollars (\$), a conversion factor of 1.42 \$/£ is employed. It should be noted that the actual costs of the two engines are higher than the values reported here, since auxiliaries, contingency funds and other fees and are not considered in the analysis. However, as this is common to both engines, a comparison between those two engines is still considered valid.

RESULTS

A comparison of the thermodynamic performance of the Up-THERM heat converter and that of an equivalent sub-critical, non-regenerative ORC engine in the selected application is presented in Table 1. For both engines, *n*-hexane has a superior thermodynamic performance to *n*-heptane in terms of power output, thermal and exergy efficiencies. Since the external temperature difference between the hot and cold heat exchangers is fixed, the oscillation amplitudes of pressure and volumetric displacement are lower for the heavier *n*-alkane in the Up-THERM heat converter. This leads to a lower heat input into the cycle and, consequently, a lower power output, since the volumetric flow rate through the hydraulic motor is reduced.

Similarly in the ORC engine, the evaporation pressure for *n*-heptane is lower than for *n*-hexane, leading to a lower power output. It can be observed that, generally, the ORC engine outperforms the Up-THERM heat converter in terms of power output and thermal efficiency, irrespective of the working fluid considered. Nevertheless, the Up-THERM demonstrates higher exergy efficiencies when the better working fluid (*n*-hexane) is selected.

Table 1. Thermodynamic performance comparison of the Up-THERM converter and ORC engine in the selected application.

Working fluid	Up-THERM			ORC		
	\dot{W}_{hm} [kW]	η_{th} [%]	η_{ex} [%]	\dot{W}_{el} [kW]	η_{th} [%]	η_{ex} [%]
<i>n</i> -hexane	2.80	7.47	38.6	5.39	14.4	26.0
<i>n</i> -heptane	0.81	3.23	17.7	3.19	12.8	23.1

The Up-THERM heat converter requires two heat exchangers, a piston/displacer cylinder arrangement, two hydraulic accumulators, two check valves and a hydraulic motor, plus pipes, connectors and auxiliaries. With *n*-hexane as the working fluid, the area of each heat exchanger amounts to $\sim 1.9 \text{ m}^2$, resulting in a cost of £38,900 for both heat exchangers. With *n*-heptane the area drops to $\sim 1.2 \text{ m}^2$, leading to a cost of £34,600.

For an indication of the costs of the displacer cylinder a piston accumulator is selected that has similar dimensions to the displacer cylinder. The piston accumulator has a cost of £220. As this is the lowest cost of any components, the influence on the overall costs is very low. In addition, two bladder accumulators with a volume of 10 L are chosen for the hydraulic accumulators in the load arrangement, which cost £1,220 each.

For the Up-THERM converter, hydraulic motors were identified for flow rates up to 200 L/min. However, the flow rate in the hydraulic circuit when using *n*-hexane is 275 L/min and when

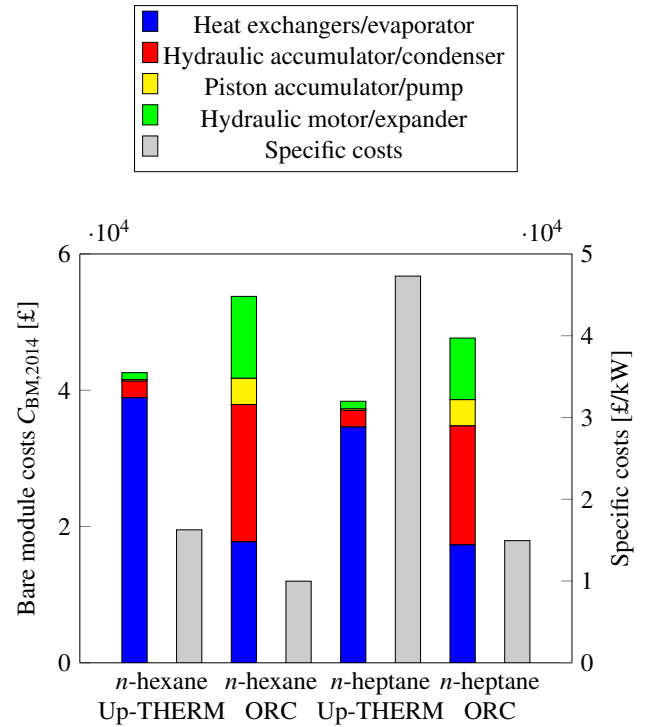


Figure 3. Total and specific costs of both engines.

using *n*-heptane it is 360 L/min, given the pressure drop across the hydraulic motor. Note that the design of the Up-THERM is optimized for maximum power output, which is achieved as a compromise in the value for the load resistance that achieves a large multiple of the load (hydraulic circuit) flow rate and pressure drop. By splitting the flow into two parallel branches, two hydraulic motors can be utilized. With *n*-hexane as the working fluid, the Flowfit FFPMT200C (£460) hydraulic motor with a maximum flow rate of 100 L/min and the Flowfit FFPMV400C (£560) with a maximum flow rate of 200 L/min were chosen; with *n*-heptane, two Flowfit FFPMV400C were chosen.

The ORC engine is also optimized for maximum net power output, and requires two heat exchangers (evaporator and condenser). The area of the evaporator is 1.3 m^2 for *n*-hexane and 1.2 m^2 for *n*-heptane, resulting in costs of £17,700 and £17,300, respectively. The area of the condenser is 2.2 m^2 for *n*-hexane and 1.3 m^2 for *n*-heptane, at a cost of £20,100 and £17,500. Furthermore, a pump is required for working fluid pressurization, at a cost of about £3,800 with either *n*-hexane or *n*-heptane. Finally, the working fluid is expanded in the expander, which contributes £12,000 (*n*-hexane) or £9,000 (*n*-heptane) to the overall costs.

From Fig. 3, it can be seen that the largest cost component in both engines is associated with the heat exchangers. However, in the Up-THERM converter those costs contribute 85% (*n*-hexane) or even 90% (*n*-heptane) of the overall costs, while in the ORC engine the share of the heat exchanger costs of the total costs is $\sim 75\%$ for both *n*-hexane and *n*-heptane. Beyond this, standard, low-cost and off-the-shelf components can be utilized for the rest of the device, which explains the very low overall cost of the Up-THERM heat converter. The fact that no pump is required, for instance, saves up to £3,800 compared to the ORC engine.

Consequently, the capital costs of the Up-THERM heat converter are 19% lower than the capital costs of the ORC engine with *n*-hexane and 21% lower with *n*-heptane as the working fluid.

In both heat conversion systems, due to the lower heat input from the heat source (and rejection to the heat sink), the heat exchanger areas are smaller when using *n*-heptane rather than *n*-hexane as the working fluid, which results in lower heat exchanger costs in both engines when *n*-heptane is employed. In the Up-THERM heat converter the flow rate through the hydraulic motor is higher when using *n*-heptane, although this only has a marginal effect on the costs as stated earlier. On the other hand, since the ORC engine power output with *n*-heptane is lower (see Table 1), a smaller expander is required, resulting in lower costs. Consequently the ORC engine with *n*-heptane as the working fluid costs £4,200 less (compared to *n*-hexane).

Finally, when considering the specific costs per unit net power output (£/kW), *n*-hexane appears as the favourable working fluid option, due to the much higher power output delivered by both engines compared to the smaller increase in cost. It can also be seen that the ORC engine has lower specific costs than the Up-THERM heat converter, which can be directly attributed to the higher power output from the ORC engine (even though the device cost of the Up-THERM is 20% lower). It is noted, however, that these costs are only capital costs and do not account for operating expenses which are expected to move the balance in favour of the Up-THERM. This is expected since the Up-THERM has fewer moving parts and seals, allowing longer maintenance cycles, and lower operating costs than the ORC engine.

CONCLUSION

A thermodynamic and economic comparison between a novel two-phase thermofluidic oscillator termed Up-THERM and an equivalent sub-critical and non-regenerative ORC engine was performed in a specific application using two *n*-alkanes as working fluids: *n*-hexane and *n*-heptane. While the net power output from the ORC engine is ~2 times higher than from the Up-THERM converter, the capital costs are approximately 20% lower for the Up-THERM heat converter. This makes the Up-THERM heat converter an attractive alternative for low-power applications, where minimizing capital costs is highly desirable.

Operating expenses were not considered in this work, which are expected to be much lower for the Up-THERM heat converter due to its simple design and minimal number of moving parts. Thus, the Up-THERM can be a viable alternative, especially in applications that require low capital and maintenance costs. This conclusion is made also on the basis that ORC systems are a mature technology with which we have decades of development and commercialization experience, whereas the Up-THERM is still in the first stages of development. In particular, the present effort was based on a pre-specified 'first-iteration' design for the Up-THERM, with pre-selected working fluids and device design that emerges as non-optimal in the chosen application.

ACKNOWLEDGEMENT

The research leading to these results has received funding from the 7th Framework Programme of the European Commission, grant agreement number 605826.

REFERENCES

- [1] Sondhauss C., Über die Schallschwingungen der Luft in erhitzten Glasröhren und in gedeckten Pfeifen von ungleicher Weite, *Annalen der Physik*, Vol. 155, No. 1, 1850, pp. 1-34
- [2] Ceperley P.H., A pistonless Stirling engine - The travelling wave heat engine, *The Journal of the Acoustical Society of America*, Vol. 66, No. 5, 1979, pp. 1508-1513
- [3] Stammers C.W., The operation of the Fluidyne heat engine at low differential temperatures, *Journal of Sound and Vibration*, Vol. 63, No. 4, 1979, pp. 507-516
- [4] Markides C.N., Osuolale A., Solanki R., and V. Stan G.B., Nonlinear heat transfer processes in a two-phase thermofluidic oscillator, *Applied Energy*, Vol. 104, 2013, pp. 958-977
- [5] Markides C.N. and Smith T.C.B., A dynamic model for the efficiency optimization of an oscillatory low grade heat engine, *Energy*, Vol., No. 12, 2011, pp. 6967-6980
- [6] Solanki R., Galindo A., and Markides C.N., Dynamic modelling of a two-phase thermofluidic oscillator for efficient low grade heat utilization: Effect of fluid inertia, *Applied Energy*, Vol. 89, No. 1, 2012, pp. 156-163
- [7] Solanki R., Mathie R., Galindo A., and Markides C.N., Modelling of a two-phase thermofluidic oscillator for low-grade heat utilisation: Accounting for irreversible thermal losses, *Applied Energy*, Vol. 106, 2013, pp. 337-354
- [8] Glushenkov M., Sprenkeler M., Kronberg A., and Kirillov V., Single-piston alternative to Stirling engines, *Applied Energy*, Vol. 97, 2012, pp. 743-748
- [9] Kirmse C.J.W., Oyewunmi O.A., Taleb A.I., Haslam A.J., and Markides C.N., Two-phase single-reciprocating-piston heat conversion engine: Non-linear dynamic modelling, *Applied Energy*, 2016, under review
- [10] Oyewunmi O.A., Kirmse C.J.W., Müller E.A., Haslam A.J., and Markides C.N., Working-fluid selection for a two-phase single-reciprocating-piston heat-conversion engine, *Applied Energy*, 2016, under review
- [11] Huang B.J. and Chuang M.D., System design of orifice pulse-tube refrigerator using linear flow network analysis, *Cryogenics*, Vol. 36, No. 11, 1996, pp. 889-902
- [12] Backhaus S. and Swift G.W., A thermoacoustic Stirling heat engine, *Nature*, Vol. 399, No. 6734, 1999, pp. 335-338
- [13] Backhaus S. and Swift G.W., A thermoacoustic-Stirling heat engine: Detailed study, *The Journal of the Acoustical Society of America*, Vol. 107, No 6, 2000, pp. 3148-3166
- [14] Solanki R., Galindo A., and Markides C.N., The role of heat exchange on the behaviour of an oscillatory two-phase low-grade heat engine, *Applied Thermal Engineering*, Vol. 53, No. 2, 2013, pp. 177-187
- [15] Oyewunmi O.A., Taleb A.I., Haslam A.J., and Markides C.N., An assessment of working-fluid mixtures using SAFT-VR Mie for use in organic Rankine cycle systems for waste-heat recovery, *Computational Thermal Sciences*, Vol. 6, No. 2, 2014, pp. 301-316
- [16] Hewitt G.F., Shires G.L., and Bott T.R., Process heat transfer, *CRC Press*, 1994
- [17] Turton R., Bailie R.C., Whiting W.B., Shaeiwitz J.A., and Bhattacharyya D., Analysis, Synthesis, and Design of Chemical Processes, *Pearson*, 2012
- [18] Seider, W.D., Seader, J.D., Lewin, D.R., Widagdo, S., Product and Process Design Principles: Synthesis, Analysis, and Evaluation, *Wiley*, 2010
- [19] <http://www.chemengonline.com/pci>, accessed 07/03/2016